inorganics

MDPI

Article

Hexacoordinate Silicon Compounds with a Dianionic Tetradentate (*N*,*N*′,*N*′,*N*)-Chelating Ligand

Daniela Gerlach [1], Erica Brendler [2] and Jörg Wagler [1,*]

[1] Institut für Anorganische Chemie, TU Bergakademie Freiberg, D-09596 Freiberg, Germany; d_gerlach@gmx.de

[2] Institut für Analytische Chemie, TU Bergakademie Freiberg, D-09596 Freiberg, Germany; erica.brendler@chemie.tu-freiberg.de

* Correspondence: joerg.wagler@chemie.tu-freiberg.de; Tel.: +49-3731-39-4343

Academic Editors: Duncan H. Gregory and Cameron Jones

Received: 17 March 2016; Accepted: 7 April 2016; Published: 14 April 2016

Abstract: In the context of our systematic investigations of penta- and hexacoordinate silicon compounds, which included dianionic tri- (*O*,*N*,*O*′; *O*,*N*,*N*′) and tetradentate (*O*,*N*,*N*,*O*; *O*,*N*,*N*′,*O*′) chelators, we have now explored silicon coordination chemistry with a dianionic tetradentate (*N*,*N*′,*N*′,*N*) chelator. The ligand [*o*-phenylene-bis(pyrrole-2-carbaldimine), H_2L] was obtained by condensation of *o*-phenylenediamine and pyrrole-2-carbaldehyde and subsequently silylated with chlorotrimethylsilane/triethylamine. Transsilylation of this ligand precursor $(Me_3Si)_2L$ with chlorosilanes $SiCl_4$, $PhSiCl_3$, Ph_2SiCl_2, $(Anis)_2SiCl_2$ and $(4\text{-}Me_2N\text{-}C_6H_4)PhSiCl_2$ afforded the hexacoordinate Si complexes $LSiCl_2$, LSiPhCl, $LSiPh_2$, $LSi(Anis)_2$ and $LSiPh(4\text{-}Me_2N\text{-}C_6H_4)$, respectively (Anis = anisyl = 4-methoxyphenyl). ^{29}Si NMR spectroscopy and, for $LSiPh_2$, $LSi(Anis)_2$ and $LSiPh(4\text{-}Me_2N\text{-}C_6H_4)$, single-crystal X-ray diffraction confirm hexacoordination of the Si atoms. The molecular structures of $LSiCl_2$ and LSiPhCl were elucidated by computational methods. Despite the two different N donor sites (pyrrole N, X-type donor; imine N, L-type donor), charge delocalization within the ligand backbone results in compounds with four similar Si–N bonds. Charge distribution within the whole molecules was analyzed by calculating the Natural Charges (NCs). Although these five compounds carry electronically different monodentate substituents, their constituents reveal rather narrow ranges of their charges (Si atoms: +2.10–+2.22; monodentate substituents: −0.54–−0.56; L^{2-}: −1.02–−1.11).

Keywords: hypercoordination; imine; pyrrole; ^{29}Si NMR spectroscopy; X-ray diffraction

1. Introduction

The coordination number of tetravalent silicon can easily be enhanced (up to five or six) with the aid of monodentate or chelating ligands. Whereas the former preferentially bind to Si atoms that carry strongly electron withdrawing groups (e.g., formation of pyridine adducts of halosilanes, Scheme 1, **A**, [1–3]), the latter offer greater opportunities of creating five- and six-coordinate silicon compounds even in case of the absence of halides from the silicon coordination sphere (e.g., pentacoordinate silicon with SiC_5 coordination sphere, **B** [4–6]; and hexacoordinate silicon with a tetradentate chelator and two Si–CH_3 groups, **C** [7]). For various reasons, such as activation of Si–X bonds by silicon hypercoordination [8–16], exploring special electronic/optical properties arising from the higher coordination number of silicon in combination with selected ligands [17–20] or the aim of creating and exploring hitherto unusual Si coordination compounds, e.g., with transition metals [21–29] or very soft Lewis bases in their ligand sphere [30–38], silicon coordination chemistry continues to be an attractive research field, reflected by frequently published research articles [39–58] and reviews [59–63]. Thus, in the context of our systematic investigations of penta- and hexacoordinate silicon compounds with

dianionic tri-(O,*N*,O′; O,*N*,*N*′) [20,64–72] and tetradentate (*O*,*N*,*N*,*O*; *O*,*N*,*N*′,*O*′) [7–11,18,19,73–77] chelators, we have now explored silicon coordination chemistry with a dianionic tetradentate (*N*,*N*′,*N*′,*N*) chelator. Thus far, macrocyclic π-conjugated (porphyrine- and phthalocyanine-type) ligands [78–81] have been explored in silicon coordination chemistry (e.g., **D** [81]), and our study aims at building a bridge between these cyclic (*N*,*N*,*N*,*N*)-chelators with essentially chemically equivalent donor atoms and "open chain" type chelators such as salen-type (*O*,*N*,*N*,*O*)-ligands (like the tetradentate ligand in **C**).

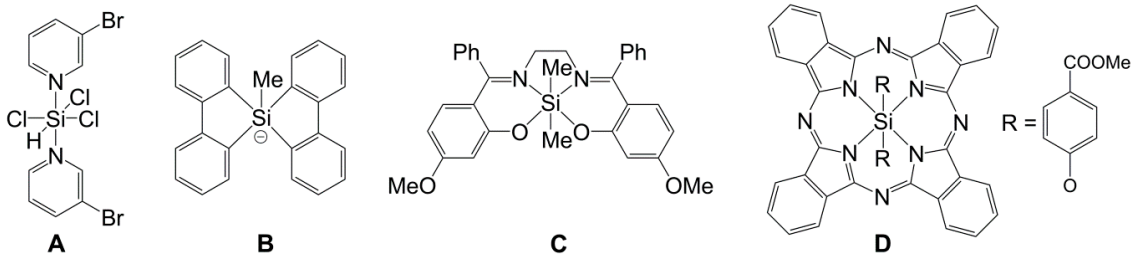

Scheme 1. Selected penta- and hexacoordinate silicon compounds with: monodentate ligands (**A**); chelating groups (**B**,**C**); and a macrocyclic (phthalocyanine) ligand (**D**).

2. Results and Discussion

2.1. Syntheses

Based on our experience with pyrrolide as anionic anchoring group in chelating ligands for Si coordination chemistry [20,64,82–84], we studied the syntheses and molecular structures of silicon compounds with a pyrrole-2-carbaldimine functionalized (*N*,*N*′,*N*′,*N*)-chelating dianionic tetradentate ligand. This ligand, H_2L, has already been reported in the literature [85] and was synthesized by condensation of *o*-phenylenediamine with two equivalents of pyrrole-2-carbaldehyde (Scheme 2). Prior to reacting with the chlorosilanes to be chelated upon substitution of two Cl atoms [$SiCl_4$, $PhSiCl_3$, Ph_2SiCl_2, $(Anis)_2SiCl_2$ and $(4\text{-}Me_2N\text{-}C_6H_4)PhSiCl_2$], H_2L was converted into its bis(trimethylsilyl) derivative $(Me_3Si)_2L$, as its conversion with further chlorosilanes (in a transsilylation reaction) produces chlorotrimethylsilane as a liquid and volatile byproduct, which allows for easy separation from the target complex. Whereas $SiCl_4$, $PhSiCl_3$, and Ph_2SiCl_2 were commercially available, $(Anis)_2SiCl_2$ and $(4\text{-}Me_2N\text{-}C_6H_4)PhSiCl_2$ were prepared from $SiCl_4$ and $PhSiCl_3$, respectively, and suitable Grignard reagents (see Experimental Section).

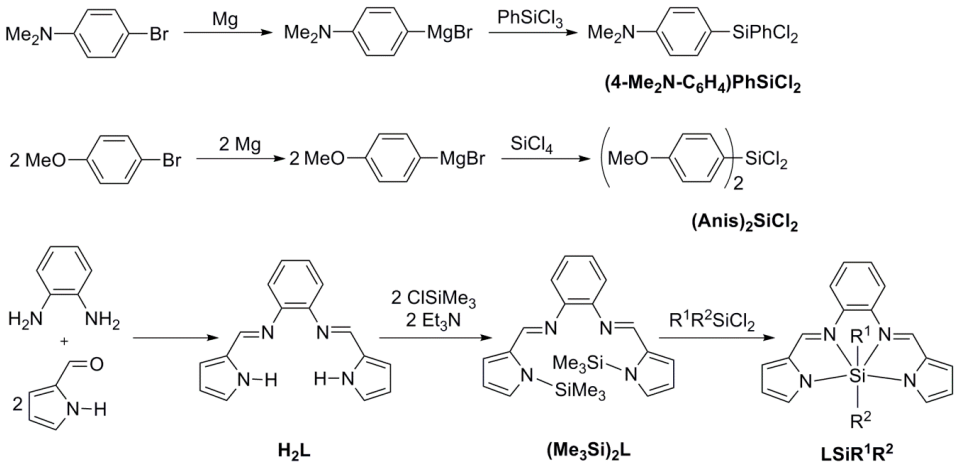

Scheme 2. Syntheses of ligands H_2L and $(Me_3Si)_2L$, silanes $(Anis)_2SiCl_2$ and$(4\text{-}Me_2N\text{-}C_6H_4)PhSiCl_2$ as well as complexes $LSiCl_2$, LSiPhCl, $LSiPh_2$, $LSi(Anis)_2$ and $LSiPh(4\text{-}Me_2N\text{-}C_6H_4)$.

Complexes $LSiCl_2$, LSiPhCl, $LSiPh_2$, $LSi(Anis)_2$ and $LSiPh(4\text{-}Me_2N\text{-}C_6H_4)$ were obtained as orange solids that exhibited poor solubility in various organic solvents. Therefore, the emphasis of characterization is put on solid-state methods (^{29}Si CP/MAS NMR spectroscopy, single-crystal X-ray diffraction) and computational methods.

2.2. Molecular Structures

The starting material $(4\text{-}Me_2N\text{-}C_6H_4)PhSiCl_2$ was obtained as a crystalline solid, therefore we determined its molecular structure in the solid state by single-crystal X-ray diffraction (Figure 1, Table 1). Because of the different substituents, the Si coordination sphere is distorted tetrahedral, with the C–Si–C angle (117.3°) significantly exceeding the tetrahedral angle. Interestingly, the Si1–C1 bond to the 4-dimethylaminophenyl group is slightly shorter than the Si1–C9 bond to the phenyl group.

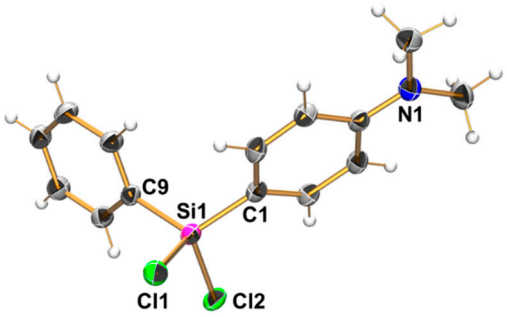

Figure 1. Molecular structure of $(4\text{-}Me_2N\text{-}C_6H_4)PhSiCl_2$ in the crystal, thermal displacement ellipsoids are drawn at the 50% probability level. Selected bond lengths (Å) and angles (deg): Si1–C1 1.841(2), Si1–C9 1.858(2), Si1–Cl1 2.083(1), Si1–Cl2 2.070(1); C1–Si1–C9 117.25(7), Cl1–Si1–Cl2 107.93(3).

Table 1. Crystallographic data from data collection and refinement for $(4\text{-}Me_2N\text{-}C_6H_4)PhSiCl_2$, $LSiPh_2 \cdot THF$, $LSi(Anis)_2 \cdot 0.5\ THF$ and $LSiPh(4\text{-}Me_2N\text{-}C_6H_4) \cdot THF$.

Parameter	$(4\text{-}Me_2N\text{-}C_6H_4)\ PhSiCl_2$	$LSiPh_2 \cdot THF$	$[LSi(Anis)_2]_2 \cdot THF$	$LSiPh(4\text{-}Me_2N\text{-}C_6H_4) \cdot THF$
Formula	$C_{14}H_{15}Cl_2NSi$	$C_{32}H_{30}N_4OSi$	$C_{64}H_{60}N_8O_5Si_2$	$C_{34}H_{35}N_5OSi$
M_r	296.26	514.69	1077.38	557.76
T (K)	150(2)	150(2)	150(2)	150(2)
λ (Å)	0.71073	0.71073	0.71073	0.71073
Crystal system	monoclinic	triclinic	monoclinic	monoclinic
Space group	$P2_1/c$	$P\text{-}1$	$P2_1/c$	Cc
a (Å)	16.6233(11)	9.7135(3)	14.3173(4)	14.5651(7)
b (Å)	7.5451(3)	14.9827(4)	18.2897(8)	22.8720(8)
c (Å)	12.2941(8)	18.4932(4)	21.3671(7)	10.4529(5)
α (°)	90	82.491(1)	90	90
β (°)	110.965(5)	83.162(1)	101.839(2)	124.370(3)
γ (°)	90	88.353(1)	90	90
V (Å^3)	1439.90(15)	2649.10(12)	5476.1(3)	2874.2(2)
Z	4	4	4	4
ρ_{calc} (g·cm^{-1})	1.367	1.290	1.307	1.289
$\mu_{MoK\alpha}$ (mm^{-1})	0.516	0.122	0.125	0.119
$F(000)$	616	1088	2272	1184
θ_{max}(°), R_{int}	30.0, 0.0500	27.0, 0.0384	28.0, 0.0496	30.0, 0.0350
Completeness	100%	98.6%	99.9%	99.9%
Reflns collected	19,787	45,819	52,823	27,745
Reflns unique	4203	11,420	13,197	7879
Restraints	0	0	0	4
Parameters	165	685	716	377
GoF	1.044	1.060	1.047	1.052
$R1$, $wR2$ [$I > 2\sigma(I)$]	0.0348, 0.0771	0.0463, 0.1140	0.0441, 0.1013	0.0331, 0.0800
$R1$, $wR2$ (all data)	0.0535, 0.0841	0.0790, 0.1241	0.0744, 0.1129	0.0381, 0.0831
Largest peak/hole (e·Å^{-3})	0.428, −0.305	0.564, −0.410	0.678, −0.590	0.307, −0.190

The diaryl substituted silicon compounds $LSiPh_2$, $LSi(Anis)_2$ and $LSiPh(4\text{-}Me_2N\text{-}C_6H_4)$ crystallized from the reaction mixture (as THF solvates) and their molecular structures were thus determined by single-crystal X-ray diffraction analyses (Figure 2, Table 1). Selected bond lengths are listed in Table 2. As $LSiCl_2$ and LSiPhCl were obtained as fine powders, even during slow formation in very dilute solutions of starting materials, and our attempts of growing crystals from other solvents failed, the molecular structures of $LSiCl_2$, LSiPhCl and $LSiPh_2$ were optimized (gas phase) at the DFT MPW1PW91/6-311G(d,p) level of theory (Figure 3). Compound $LSiPh_2$ thus serves as our internal reference for the reliability of the computed molecular structure as an experimentally determined structure of this compound is available for comparison. Selected bond lengths of these molecules are also listed in Table 2.

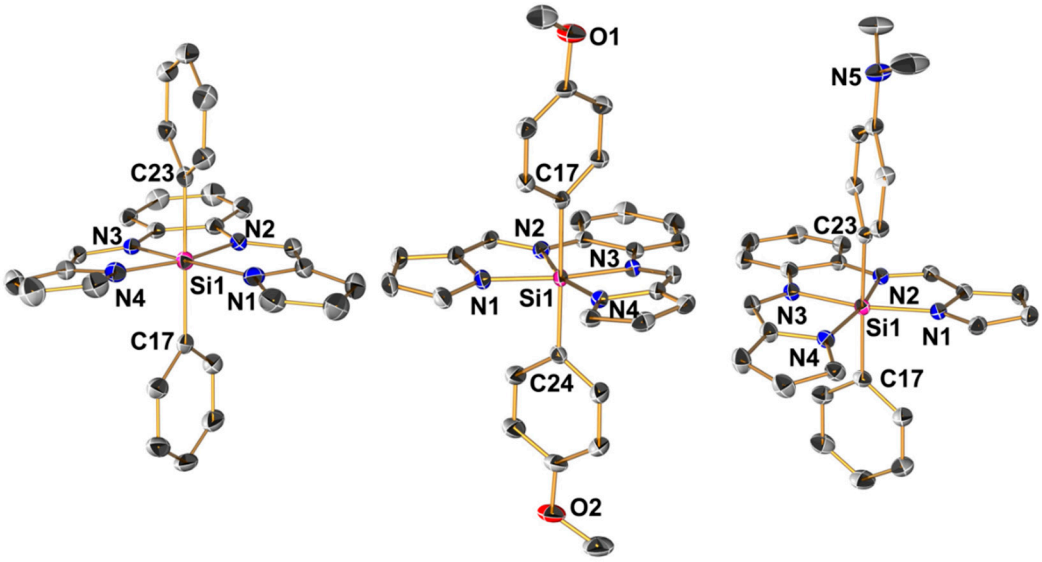

Figure 2. Molecular structures of (from left) $LSiPh_2$, $LSi(Anis)_2$ and $LSiPh(4\text{-}Me_2N\text{-}C_6H_4)$ in their crystal structures (heteroatoms and Si-bound C atoms labeled, H-atoms, solvent molecules and second independent molecule of the asymmetric unit of $LSiPh_2$ and $LSi(Anis)_2$ are omitted).

Table 2. Bond lengths (Å) in the Si coordination spheres of the hexacoordinate Si complexes discussed in this paper.

Bond	$LSiPh(4\text{-}Me_2N\text{-}C_6H_4)$	$LSi(Anis)_2$ [1]	$LSiPh_2$ [1]	$LSiPh_2$ [2]	LSiPhCl [2]	$LSiCl_2$ [2]
Si–C	1.994(1) [3] 1.964(1) [4]	1.995(2) 1.974(2)	1.983(2) 1.977(2)	1.967 1.967	1.949 -	- -
$Si–N_{pyrrole}$	1.900(1) 1.890(1)	1.904(1) 1.896(1)	1.882(2) 1.890(1)	1.948 1.948	1.877 1.877	1.851 1.852
$Si–N_{imine}$	1.919(1) 1.905(1)	1.923(2) 1.915(1)	1.906(1) 1.908(1)	1.933 1.933	1.906 1.906	1.892 1.892
Si–Cl	- -	- -	- -	- -	2.294 -	2.227 2.228

[1] Data taken from one of the two crystallographically independent molecules (the molecule shown in Figure 2). The other molecule in the asymmetric unit exhibits very similar bond lengths; [2] from optimized molecular structures (see Figure 3); [3] C of the phenyl group; [4] C of the *p*-dimethylaminophenyl group.

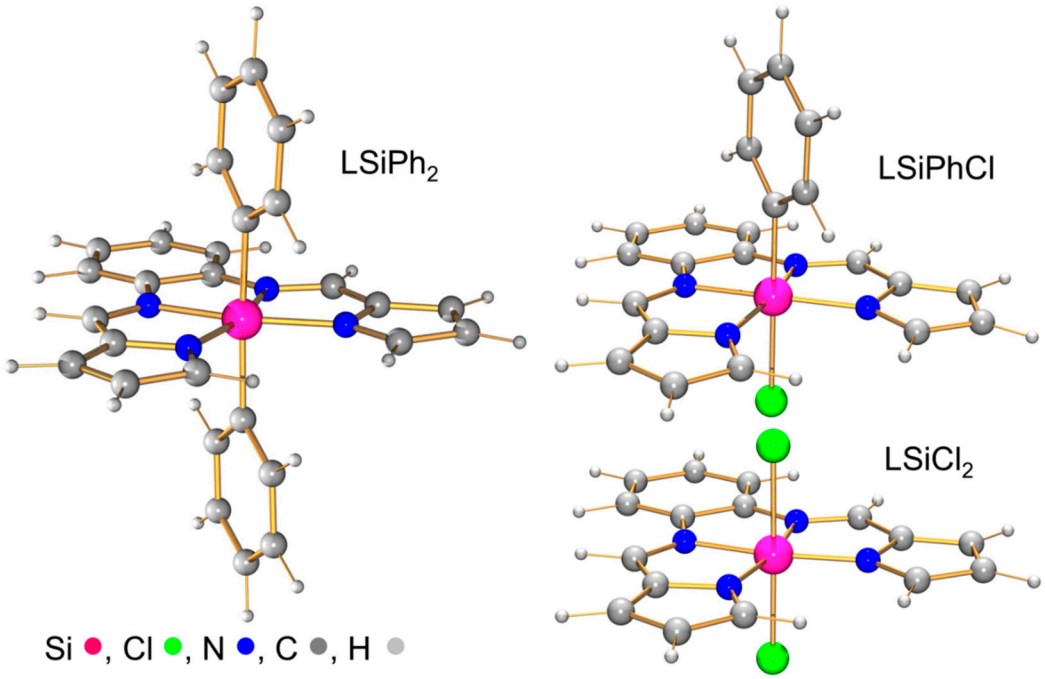

Figure 3. Molecular structures of $LSiPh_2$, LSiPhCl and $LSiCl_2$ optimized at the MPW1PW91/6-311G(d,p) level.

In the solid-state compounds $LSiPh_2$, $LSi(Anis)_2$ and $LSiPh(4\text{-}Me_2N\text{-}C_6H_4)$ exhibit *trans*-disposed Si–C bonds, which appears reasonable because of the rigidity of the tetradentate chelator. Therefore, the molecular structures of $LSiCl_2$, LSiPhCl and $LSiPh_2$ were optimized starting from a model with *trans*-disposed monodentate substituents. Direct comparison of the bond lengths found for $LSiPh_2$ in the solid state and predicted by computational methods shows satisfactory agreement, even though the computational analysis appears to underestimate the bond strength to the tetradentate ligand (it predicts longer Si–N bonds) and the weakening of the Si–C bonds resulting therefrom. Thus, we only interpret the trends observed in the optimized molecular structures rather than interpreting the absolute bond length values.

Both in the series of crystallographically determined molecular structures and in the series of computed structures we find systematic shortening of the Si–N bonds upon lowering the electron releasing power or increasing the electron withdrawing power of the monodentate substituents. Even though the experimental data confirm slightly longer $Si–N_{imine}$ bonds for $LSiPh_2$, whereas computational analysis predicts slightly longer $Si–N_{pyrrole}$ bonds, these two kinds of bonds exhibit only marginal bond length differences (despite their formally different character as dative bond from an imine N atom and a covalent bond from a pyrrole N atom). Thus, the tetradentate ligand under investigation reveals nearly perfect delocalization of its anionic charges over the chemically different nitrogen donor atoms (Scheme 3). In this regard, its imine-pyrrolide donor moiety, at least in hexacoordinate Si complexes, reflects the intermediate situation of what we had encountered with the pentacoordinate Si complexes **E** and **F** [64] (Scheme 3), each of which prefers one of the resonance contributions, depending on the situation of the imine and pyrrolide donor sites within the distorted trigonal bipyramidal coordination sphere (axial *vs.* equatorial positions). In this regard, compound $LSiPh_2$ is related to (tetraphenylporphyrine)$SiPh_2$ [79], which also has a delocalized π-system and similar Si–N bond lengths. The Si–C bonds in $LSiPh_2$ (1.98 Å), however, are slightly longer than those in the porphyrine complex (1.95 Å), whereas the Si–N bonds (1.89, 1.91 Å) are shorter than in the porphyrine complex (1.97 Å). We attribute this difference (shorter Si–N bonds in $LSiPh_2$ and pronounced Si–C bond lengthening resulting therefrom) to the smaller chelate size, *i.e.*, five-membered rings in $LSiPh_2$, whereas in porphyrin complexes six-membered rings are encountered.

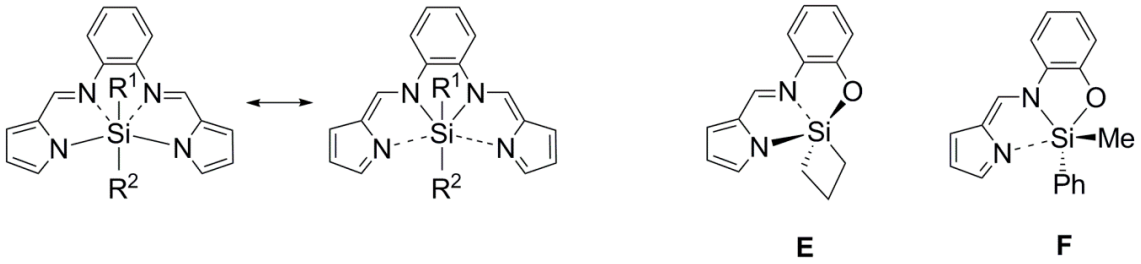

Scheme 3. Resonance structures for the interpretation of the Si–N bonding situation in the hexacoordinate Si complexes discussed in this paper and two examples (**E** and **F**) of compounds that exhibit pronounced contributions of the one or the other mesomeric form.

Moreover, for the two complexes bearing two different monodentate substituents (LSiPh(4-Me_2N-C_6H_4) and LSiPhCl) we observe pronounced bond strengthening of the Si–C bond to the more electron releasing group, whereas the bond to the *trans*-disposed rather electron withdrawing group (Ph in LSiPh(4-Me_2N-C_6H_4) , Cl in LSiPhCl) is significantly weakened relative to the corresponding bonds in the symmetrically substituted complexes $LSiPh_2$ and $LSiCl_2$, respectively.

2.3. ^{29}Si NMR

Compounds $LSiPh_2$, $LSi(Anis)_2$ and LSiPh(4-Me_2N-C_6H_4) exhibited sufficient solubility in DMSO for NMR spectroscopic investigation. Their ^{29}Si NMR shifts (δ −165.3, −165.1, and −164.4 ppm, respectively) are very similar to one another and are characteristic of hexacoordinate Si complexes. Moreover, for $LSiPh_2$, LSiPhCl and $LSiCl_2$ solid-state ^{29}Si NMR (cross-polarization magic angle spinning, CP/MAS), spectra were recorded and isotropic chemical shifts δ_{iso} characteristic of hexacoordinate Si were recorded (−164.3, −145.2, and −175.3, respectively). Comparison of the ^{29}Si NMR shift of $LSiCl_2$ with the ^{29}Si NMR shifts of porphyrine-$SiCl_2$ complexes (*ca.* −220 ppm [78]) reveals a clear difference between these two classes of silicon compounds on the NMR spectroscopic level. Comparison of the solution state and solid-state ^{29}Si NMR shift of $LSiPh_2$ indicates that the hexacoordination found in the solid state is retained in solution, hence, dynamic equilibria between hexa- and tetracoordinate Si complexes, which would shift the ^{29}Si resonance to lower field, do not play a significant role. Interestingly, for LSiPhCl we observe a surprisingly lowfield shifted ^{29}Si signal, although stepwise substitution of Ph for Cl should cause upfield shifts of the ^{29}Si signal, as shown for the series $(oxinate)_2SiPh_2$ (δ_{iso} −137 ppm), $(oxinate)_2SiPhCl$ (δ_{iso} −152 ppm), $(oxinate)_2SiCl_2$ (δ_{iso} −159 ppm) [86]. We attribute the downfield shift observed for LSiPhCl to a partial transition towards pentacoordinate Si in terms of Si–Cl bond lengthening (towards ionic Si–Cl bond dissociation). Kost *et al.* [87] have already reported that ionic dissociation of Si–Cl bonds is favored upon replacing an $SiCl_2$ moiety of a hexacoordinate Si complex by an SiCl(alkyl) moiety. Apparently, a phenyl substituent can serve the same purpose of supporting this ionic dissociation, and the Si–Cl bond in the optimized molecular structure of LSiPhCl (2.29 Å, *vide supra*) also hints at significant Si–Cl bond lengthening (with respect to the Si–Cl bonds of $LSiCl_2$, 2.23 Å), supported by shortening of the *trans*-disposed Si–C bond (1.95 Å) with respect to the Si–C bonds in $LSiPh_2$ (1.97 Å). For the $(oxinate)_2SiPh_nCl_{2-n}$ system this Si–Cl bond lengthening has not been observed (Si–Cl 2.19 Å for n = 0, 2.20 Å for n = 1).

As for compound $LSiPh_2$, both solid-state ^{29}Si NMR data and crystallographically determined molecular structure are available, we have determined the chemical shift anisotropy (CSA) tensor both from CP/MAS spinning side bands (Figure 4) and quantum chemical calculations based on the solid-state molecular structure (atomic coordinates from the crystal structure were used, only coordinates of H atoms were subject to optimization prior to calculating the ^{29}Si CSA tensor). As the computationally obtained data are in good agreement with the experimental values (Table 3), they allow for assignment of the directions of the CSA tensor principal components within the molecule (Figure 4).

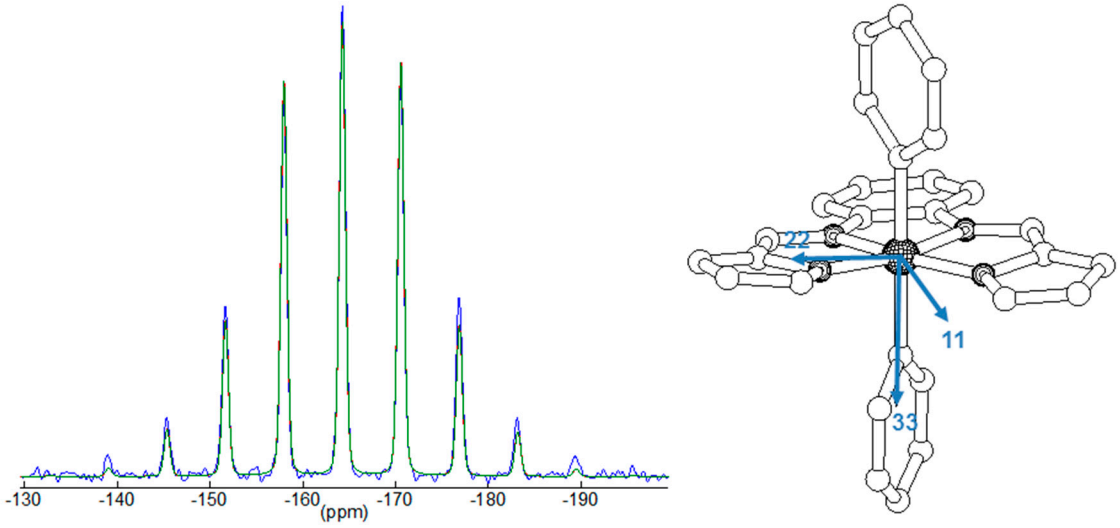

Figure 4. ^{29}Si CP/MAS NMR spinning side band spectrum of $LSiPh_2$ (ν_{spin} = 500 Hz) (**left**), and directions of the principal components δ_{11}, δ_{22} and δ_{33} of the CSA tensor in the molecule (**right**).

Table 3. Parameters of the ^{29}Si NMR CSA tensor (isotropic chemical shift δ_{iso}; principal components δ_{11}, δ_{22}, δ_{33}; span Ω; skew κ, according to the Herzfeld–Berger notation [88,89]) for $LSiPh_2$ obtained from a CP/MAS spectrum ($LSiPh_{2exp}$) and from quantum chemical calculations ($LSiPh_{2calc}$) as well as experimentally obtained CSA tensor data of a hexacoordinate (*O*,*N*,*N*,*O*)$SiPh_2$ complex of the chelating ligand shown in Scheme 1 for compound **C**.

Parameter	$LSiPh_{2exp}$	$LSiPh_{2calc}$	(*O*,*N*,*N*,*O*)$SiPh_2$
δ_{iso} (ppm)	−164.3	−166.9	−177.7
δ_{11} (ppm)	−147.3	−149.9	−162.8
δ_{22} (ppm)	−164.6	−168.1	−174.3
δ_{33} (ppm)	−181.0	−182.9	−196.0
Ω (ppm) [1]	33.7	33.0	33.2
κ [2]	−0.03	−0.11	0.31

[1] $\Omega = \delta_{11} - \delta_{33}$; [2] $\kappa = 3(\delta_{22} - \delta_{iso})/\Omega$.

In accord with the CSA data of a somewhat related complex, (*O*,*N*,*N*,*O*)$SiPh_2$ with *trans*-disposed Si–C bonds and an equatorial dianionic tetradentate salen-type ligand [7] (the same ligand as for compound **C** in Scheme 1), pronounced shielding (direction δ_{33}) is found along the C–Si–C axis, whereas components δ_{11} and δ_{22} are located in the idealized plane of the tetradentate chelating ligand. Interestingly, the change of the tetradentate chelator exerts similar influence on all principal components, hence, the span Ω of the CSA tensor is essentially the same and even the skew κ is hardly altered. In this regard, we find that the directional electronic effects of the (*N*,*N*′,*N*′,*N*) ligand used in this study on the ^{29}Si NMR shift are very similar to those of salen type (*O*,*N*,*N*,*O*) ligands.

2.4. Light Sensitivity

For diorganosilicon complexes with tetradentate salen-type ligands we have reported migration of one of the Si-bound substituents to an imine C-atom (with formation of pentacoordinate Si complexes) upon irradiation with UV (Scheme 4, left) [9,11,77], and we have observed similar behavior for silacycloalkanes with two (*O*,*N*) bidentate oxinate ligands $(oxinate)_2Si(CH_2)_n$ (n = 3–6) [90]. The herein reported hexacoordinate diorgano Si complexes $LSiPh_2$, $LSi(Anis)_2$ and $LSiPh(4\text{-}Me_2N\text{-}C_6H_4)$ are also sensitive to light and have thus been synthesized in the dark. Upon exposure to visible light or upon irradiation with UV the initially orange compounds turn dark red. Deliberate exposure of THF solutions of $LSiPh_2$, $LSi(Anis)_2$ and $LSiPh(4\text{-}Me_2N\text{-}C_6H_4)$ to UV thus resulted in the formation

of dark red solutions. In contrast to our previous studies of complexes with (*O*,*N*) and (*O*,*N*,*N*,*O*) chelated diorgano silicon compounds, UV-induced rearrangement of the herein reported compounds of the type LSiRR′ seems to produce complex mixtures of polymeric products rather than affording well-defined monomolecular complexes. This was concluded from the absence of detectable ^{29}Si NMR signals from solutions of the product mixtures. The same observations were made under less vigorous conditions, *i.e.*, upon stirring THF solutions of these complexes in Schenk tubes out of regular glassware exposed to the visible light of the laboratory environment. Nonetheless, rearrangement of one Si-bound aryl group with migration to an imine C atom (according to Scheme 4, right) should be thermodynamically allowed, as we could show by quantum chemical calculations. The proposed rearrangement products (L^RSiR') are thermodynamically more stable by about 35 kcal·mol^{-1}. Atomic coordinates of the optimized molecular structures of compounds LSiRR′ and L^RSiR' can be found in the supporting information.

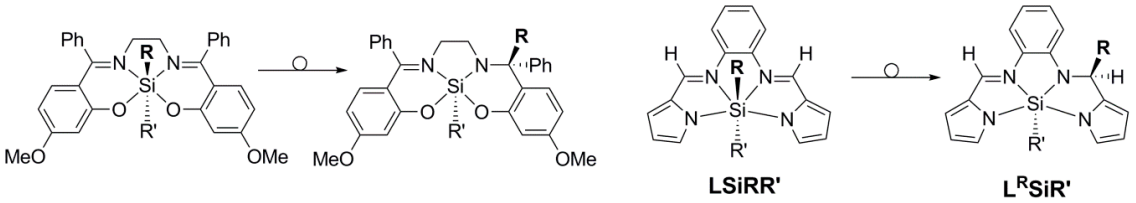

Scheme 4. UV induced rearrangement of an Si-bound hydrocarbyl group in hexacoordinate Si complexes (migration to an imine C atom) observed for complexes of salen-type ligands (**left**) and calculated to be thermodynamically allowed for the herein reported diarylsilicon complexes LSiRR′ (**right**). Rearrangement energies calculated for the following combinations R,R′ are: Ph,Ph: −34.1 kcal·mol^{-1}; Anis,Anis: −34.7 kcal·mol^{-1}; (4-Me$_2$N-C$_6$H$_4$),Ph: −35.6 kcal·mol^{-1}; Ph,(4-Me$_2$N-C$_6$H$_4$): −34.4 kcal·mol^{-1}.

2.5. Charge Distribution

The different combinations of Si-bound monodentate substituents in the herein discussed complexes gave rise to different Si–N separations within the tetradentate (*N*,*N*′,*N*′,*N*)-chelate and we found the (expected) general trend of shortening of Si–N bonds upon enhancing the electron withdrawing capabilities of the monodentate Si-bound substituents. In order to shed some light on these electrostatic interaction, we have employed quantum chemical calculations of the Natural Charges (NCs) of the atoms of all herein discussed complexes LSiRR′. A comparison of the sum of NCs for the molecular fragments L, Si, R and R′ is listed in Table 4. Interestingly, the NC of the silicon atom hardly changes upon alteration of the Si-bound monodentate substituents. Replacing aryl substituents by Cl atoms causes lowering of the Si atom's positive NC (especially for LSiCl$_2$). Comparison of the Cl atoms' NCs in LSiPhCl and LSiCl$_2$ indicates that in the latter the Cl atoms carry a less pronounced negative charge (which we attribute to the shorter Si–Cl bond). Thus, we attribute the lowering of the Si atom's NC in LSiCl$_2$ to charge compensation effects caused by the closer proximity of Si and its monodentate substituents. In the same manner, the NCs of the tetradentate ligands L become less negative as the Si–N bonds are getting shorter (*i.e.*, from LSi(aryl)$_2$ via LSiPh to LSiCl$_2$). Inter-ligand push-pull effects (*i.e.*, lowering of one ligand's charge while enhancing the other ligand's charge) are not observed. This is most obvious for LSiPh(4-Me$_2$N-C$_6$H$_4$), in which the two electronically different aryl groups still carry similar NCs, despite the electron releasing NMe$_2$ substituent. The slightly less pronounced NC of the 4-Me$_2$N-C$_6$H$_4$ group can again be interpreted as a result of slightly better charge compensation caused by the shorter Si–C bond, whereas the NC of the *trans*-disposed Ph group does not change (with respect to the NCs of the aryl groups in LSiPh$_2$ and LSi(Anis)$_2$).

Table 4. Natural Charges (NCs) of ligand L, Si and the monodentate substituents of the hexacoordinate Si complexes discussed in this paper.

Moiety	LSiPh(4-Me_2N-C_6H_4)	$LSi(Anis)_2$	$LSiPh_2$	LSiPhCl	$LSiCl_2$
Si	2.216	2.209	2.215	2.186	2.102
L	−1.110	−1.107	−1.100	−1.051	−1.023
R	−0.559	−0.556	−0.557	−0.562	−0.539
	(Ph)	(Anis)	(Ph)	(Ph)	(Cl)
R′	−0.547	−0.546	−0.557	−0.572	−0.540
	(4-Me_2N-C_6H_4)	(Anis)	(Ph)	(Cl)	(Cl)

3. Experimental Section

3.1. General Considerations

Chemicals commercially available were used as received without further purification. 4-Bromoanisole and 4-bromo-*N*,*N*-dimethylaniline were stored over activated molecular sieves (3 Å) for at least 7 days. THF, diethyl ether, toluene and triethylamine were distilled from sodium benzophenone. Triethylamine, DMSO and chloroform were stored over activated molecular sieves (3 Å) and THF, diethyl ether and toluene were stored over sodium wire under argon atmosphere. All reactions were carried out under an atmosphere of dry argon utilizing standard Schlenk techniques. H_2L was synthesized according to a literature procedure [85]. Solution NMR spectra (^1H, ^{13}C, ^{29}Si) were recorded on a Bruker DPX 400 MHz spectrometer (Me_4Si as internal standard). ^{29}Si (CP/MAS) NMR spectra were recorded on a Bruker Avance 400 WB spectrometer with 7 mm zirconia (ZrO_2) rotors and KelF inserts. Elemental analyses were performed on an Elementar Vario MICRO cube. Single-crystal X-ray diffraction data were collected on a Bruker APEX2 CCD ($LSiPh_2 \cdot THF$) and a STOE IPDS-2T diffractometer ((4-Me_2N-C_6H_4)$PhSiCl_2$, $[LSi(Anis)_2]_2 \cdot THF$, LSiPh(4-$Me_2N$-$C_6H_4$)$\cdot THF$) using Mo K$\alpha$-radiation. The structures were solved by direct methods using SHELXS-97 and refined with the full-matrix least-squares methods of F^2 against all reflections with SHELXL-97 [91–93]. All non-hydrogen atoms were anisotropically refined. Hydrogen atoms were isotropically refined in idealized position (riding model). Graphics of molecular structures were generated with ORTEP-3 [94] and POV-Ray 3.62 [95]. CCDC 999945 ($LSi(Anis)_2 \cdot 0.5 \cdot THF$), 999946 ($LSiPh_2 \cdot THF$), 999947 (Ph(4-$Me_2N$-$C_6H_4$)$SiCl_2$) and 999948 (LSiPh(4-$Me_2N$-$C_6H_4$)$\cdot THF$) contain the supplementary crystal data for this article. These data can be obtained free of charge from the Cambridge Crystallographic Data Centre via www.ccdc.cam.ac.uk/data_request/cif. Computational analyses were performed with Gaussian 09 [96]. All molecules were optimized using the DFT-MPW1PW91 [97–100] functional and the 6-311G(d,p) [101,102] basis set. The single-point energies and NBO analyses [103–109] have been calculated at the MP2/cc-pVTZ level [110–119]. Color graphics (Figures S1–S9) and atomic coordinates (Tables S1–S9) of the optimized molecular structures are available in the supplementary material. Prior to calculations of ^{29}Si NMR shifts (for the molecular structures obtained by X-ray crystallography) the positions of the H atoms were optimized (using the DFT-MPW1PW91 functional and the 6-311G(d,p) basis set), and the reference molecule $SiMe_4$ was (fully) optimized at the same level of theory as the target molecule. The NMR calculation of the molecules and the reference molecule were obtained with DFT-B3LYP/6-311G(d,p) [120].

3.2. Syntheses

Ph(4-Me_2N-C_6H_4)$SiCl_2$. Magnesium turnings (13.5 g, 0.557 mol) in THF (40 mL) were activated with a small amount of iodine at room temperature. To this mixture a small amounts (*ca.* 2 mL) of a solution of *p*-bromo-*N*,*N*-dimethylaniline (22.2 g, 0.185 mol) in THF (20 mL) was added via dropping funnel. The remaining aniline solution was then diluted further with THF (80 mL) and added dropwise. After completion of addition of *p*-bromo-*N*,*N*-dimethylaniline solution (about 60 min), the reaction mixture was stirred for another 5 h at room temperature. After storage at room temperature over

night the Grignard reagent was transferred via cannula into a dropping funnel and the residual magnesium was washed with THF (3 × 30 mL) and dried *in vacuo* (converted Magnesium 2.97 g, 0.122 mol, 66% *p*-bromo-*N*,*N*-dimethylaniline reacted). The Grignard reagent was added dropwise (within 3 h) to a solution of phenyltrichlorsilane (25.3 g, 0.120 mol) and diethyl ether (60 mL) under vigorous stirring. The mixture was stored at room temperature for 5 d, whereupon the solvent was removed under reduced pressure (condensation into a cold trap). The residue was refluxed in toluene (80 mL) for 2 h and then cooled to 0 °C. The solid precipitate was filtered off and washed with toluene (5 × 20 mL). From the combined filtrate and washings the volatiles were condensed in a cold trap under reduced pressure. The residue was distilled at 3.8–4.5 × 10^{-2} Torr (b.p. = 190–192 °C). The liquid product solidified at room temperature within 8 h. Yield: 9.27 g (31.3 mmol, 17% based on the p-bromo-*N*,*N*-dimethylaniline used). Elemental analysis for $C_{14}H_{15}Cl_2NSi$ (296.26 g· mol^{-1}): C, 56.76%; H, 5.10; N, 4.73; found C, 53.61%; H, 5.45%; N, 4.25%. The composition found indicates complete reaction with water during sample preparation, it fits the formula [Ph(*p*-HMe_2N-C_6H_4)SiClOH]Cl. Calculated for $C_{14}H_{17}Cl_2NOSi$ (314.28 g· mol^{-1}): C, 53.50%; H, 5.45%; N, 4.46. ^{1}H NMR (400.1 MHz, $CDCl_3$): δ (ppm) 3.00 (s, 6H, –CH_3), 6.71–6.72 (m, 2H, aryl), 7.40–7.48 (mm, 3H, aryl), 7.57–7.59 (m, 2H, aryl), 7.75–7.77 (m, 2H, aryl); ^{13}C{^{1}H} NMR (100 MHz, $CDCl_3$): δ (ppm) 47.3 (–NMe_2), 111.4, 115.9, 128.2, 131.4, 133.0, 134.1, 135.4, 152.4 (aryl); ^{29}Si{^{1}H} NMR (79.5 MHz, $CDCl_3$): δ (ppm) 6.2.

(Anis)$_2$SiCl$_2$. (With reference to a literature method [121]): Magnesium turnings (10.6 g, 0.437 mol) in 30 mL diethyl ether were activated with a small amount of iodine. To this mixture only 1–2 mL of the total amount of *p*-bromoanisole (27.0 g, 0.144 mol) was added. The remaining *p*-bromoanisole was dissolved in diethyl ether (60 mL) and added dropwise to the vigorously stirring mixture (within 1.5 h). Thereafter, more diethyl ether (50 mL) was added and the mixture was stirred under reflux for 45 min and then cooled to room temperature. The Grignard reagent solution was transferred into a dropping funnel (via cannula), the residual magnesium was washed with diethyl ether (4 × 10 mL) and the washings were added to the Grignard solution. The residual magnesium was then washed with THF (40 mL) and dried in vacuum to find a weight difference of converted Magnesium of 3.48 g, 0.143 mol, 99% according to the *p*-bromoanisole used. The Grignard reagent was added dropwise (within 2 h) to a vigorously stirring solution of $SiCl_4$ (12.2 g, 0.0716 mol) and diethyl ether (20 mL) at 0 °C. Thereafter, this solution was stored at room temperature overnight (10 h), whereupon the solvent was removed under reduced pressure (condensation into a cold trap). The white residue was stirred with hexane (150 mL), filtered off and washed with hexane (40 mL). From the filtrate and washings the solvent was removed under reduced pressure (condensation into a cold trap) and the residual colorless oil was distilled under reduced pressure to yield (Anis)$SiCl_3$ (6.53 g, 27.0 mmol, 19%) at 70 °C, 3.3 × 10^{-2} Torr and (Anis)$_2SiCl_2$ (2.93 g, 9.36 mmol, 13%) at 160–161 °C, 1.8–2.0 × 10^{-2} Torr. **(Anis)SiCl$_3$**: ^{1}H NMR (400 MHz, $CDCl_3$): δ (ppm) 3.45 (s, 6H, –OCH_3), 6.99 (d, *J* = 8.6 Hz, 2H, aryl), 7.73 (d, *J* = 8.6 Hz, 2H, aryl). ^{13}C{^{1}H} NMR (100 MHz, $CDCl_3$): δ (ppm) 55.3 (–CH_3), 114.2, 122.5, 135.1, 163.1 (aryl); ^{29}Si{^{1}H} NMR (79,5 MHz, $CDCl_3$): δ (ppm) −1.1. **(Anis)$_2$SiCl$_2$**: ^{1}H NMR (400 MHz, $CDCl_3$): δ (ppm) 3.84 (s, 6H, –OCH_3), 6.97 (d, *J* = 8.70 Hz, 4H, aryl), 7.67 (d, *J* = 8.70 Hz, 4H, aryl). ^{13}C{^{1}H} NMR (100 MHz, $CDCl_3$): δ (ppm) 55.2 (–CH_3), 114.0, 123.3, 135.9, 162.3 (aryl). ^{29}Si{^{1}H} NMR (79.5 MHz, $CDCl_3$): δ (ppm) 5.9.

LSiCl$_2$. A solution of H_2L (0.60 g, 2.29 mmol) and triethylamine (0.93 g, 9.21 mmol) in THF (7.5 mL) was stirred at room temperature, and chlorotrimethylsilane (0.60 g, 5.53 mmol) in THF (2.5 mL) was added dropwise via syringe. The yellow suspension thus obtained was heated to and stirred at 50 °C (3 h) and cooled to room temperature. Thereafter, the triethylamine hydrochloride precipitate was filtered off and washed with THF (3 mL). From the combined filtrate and washings the solvent was removed under reduced pressure (condensation into a cold trap), the orange residue was dissolved in chloroform (5 mL) and a solution of $SiCl_4$ (0.41 g, 2.41 mmol) in chloroform (2 mL) was added dropwise via syringe. Within few seconds a precipitate formed. The mixture was stored at 6 °C (2 d), whereupon the solid was filtered off, washed with chloroform (0.5 mL) and dried in vacuum. Yield: 0.90 g (2.09 mmol, 82%) of $LSiCl_2 \cdot CHCl_3$. This compound is basically insoluble in common

solvents such as hexane, diethyl ether, THF, toluene and DMSO. Elemental analysis for $C_{17}H_{13}N_4SiCl_5$ (478.66 g·mol^{-1}): C, 42.66%; H, 2.74; N, 11.70%; found C, 42.72; H, 3.17%; N, 11.70%. $^{29}Si\{^1H\}$ CP/MAS NMR (79.5 MHz): δ_{iso} (ppm) −175.3.

LSiPhCl. A solution of H_2L (0.50 g, 1.91 mmol) and triethylamine (0.58 g, 5.74 mmol) in THF (5 mL) was stirred at room temperature, and chlorotrimethylsilane (0.50 g, 4.61 mmol) in THF (2.5 mL) was added dropwise via syringe. The yellow suspension thus obtained was heated to and stirred at 50 °C (3 h) and cooled to room temperature. Thereafter, the triethylamine hydrochloride precipitate was filtered off and washed with THF (2 mL). From the combined filtrate and washings the solvent was removed under reduced pressure (condensation into a cold trap). The orange residue was dissolved in chloroform (5 mL) and a solution of phenyltrichlorsilane (0.42 g, 1.99 mmol) in THF (2.5 mL) was added dropwise via syringe. Within few seconds an orange precipitate formed. The mixture was stored at 6 °C (1 d), whereupon the solid product was filtered off, washed with THF (0.5 mL) and dried in vacuum. Yield: 0.49 g (1.04 mmol, 54%) of LSiClPh·THF. This compound is basically insoluble in common solvents such as hexane, diethyl ether, THF, toluene and DMSO. Elemental analysis for $C_{26}H_{25}N_4OSiCl$ (473.04 g·mol^{-1}): C, 66.02%; H, 5.33%; N, 11.84%; found C, 65.98%; H, 5.51%; N, 11.79%. $^{29}Si\{^1H\}$ CP/MAS NMR (79.5 MHz): δ_{iso} (ppm) −145.2.

LSiPh$_2$. A solution of H_2L (2.00 g, 7.63 mmol) and triethylamine (3.85 g, 38.1 mmol) in THF (35 mL) was stirred at room temperature, and chlorotrimethylsilane (2.48 g, 22.9 mmol) in THF (5 mL) was added dropwise via syringe. The yellow suspension thus obtained was heated to and stirred at 50 °C (4 h) and cooled to room temperature. Thereafter, the triethylamine hydrochloride precipitate was filtered off and washed with THF (10 mL). From the combined filtrate and washings the solvent was removed under reduced pressure (condensation into a cold trap). The orange residue was dissolved in THF (10 mL). In the dark a solution of diphenyldichlorsilane (2.03 g, 8.02 mmol) in THF (3 mL) was added quickly (with stirring) and the solution was then stored at room temperature in the dark for 6 days. The orange crystals obtained were filtered off, washed with THF (5 mL) and briefly dried in vacuum. Yield: 2.86 g (5.56 mmol, 73%) of LSiPh$_2$·THF. Elemental analysis for $C_{32}H_{30}N_4OSi$ (514.69 g·mol^{-1}): C, 74.67%; H, 5.87%; N, 10.89%; found C, 74.14%; H, 5.56%; N, 10.81%. ^1H NMR (400 MHz, DMSO-d_6): δ (ppm) 6.46–6.47 (m, 2H, aryl), 6.66–6.70 (m, 6H, aryl), 6.80–6.82 (m, 4H, aryl), 6.91–6.92 (m, 2H, aryl), 7.42–7.44 (m, 2H, aryl), 7.99–8.00 (m, 2H, aryl), 8.29 (s, 2H, aryl), 9.05 (s, 2H, –N=CH–); $^{13}C\{^1H\}$ NMR (100 MHz, DMSO-d_6): δ (ppm) 115.7, 115.8, 118.9, 124.4, 126.3, 127.3, 132.0, 134.4, 134.6, 135.4, 141.6 (aryl), 160.4 ppm (–N=CH–); $^{29}Si\{^1H\}$ NMR (79.5 MHz, DMSO-d_6): δ (ppm) −165.3.

LSi(Anis)$_2$. A solution of H_2L (0.80 g, 3.05 mmol) and triethylamine (1.00 g, 9.22 mmol) in THF (10 mL) was stirred at room temperature, and chlorotrimethylsilane (1.24 g, 12.3 mmol) in THF (4 mL) was added dropwise via syringe. The yellow suspension thus obtained was heated to and stirred at 50 °C (4 h) and cooled to room temperature. Thereafter, the triethylamine hydrochloride precipitate was filtered off and washed with THF (5 mL). From the combined filtrate and washings the solvent was removed under reduced pressure (condensation into a cold trap). The orange residue was dissolved in THF (7 mL). In the dark 2.04 g of a 50% solution of $(Anis)_2SiCl_2$ in hexane (corresponding to 1.02 g, 3.20 mmol) was added quickly with stirring and the solution was stored at room temperature in the dark for 6 days. The orange crystals obtained were filtered off, washed with THF (2 × 1.5 mL) and briefly dried in vacuum. Yield: 0.91 g (1.69 mmol, 55%) of LSi(Anis)$_2$·0.5THF. This composition was concluded from the crystallographic data. ^1H NMR data and elemental analysis suggest a somewhat higher THF content (0.7 THF). Elemental analysis for $C_{32.8}H_{31.6}N_4O_{2.7}Si$ (553.11 g·mol^{-1}): C, 71.22%; H, 5.76%; N, 10.13%; found C, 70.64%; H, 6.06%; N, 10.50%. ^1H NMR (400 MHz, DMSO-d_6): δ (ppm) 3.45 (s, 6H, –O–CH_3), 6.25–6.27 (m, 4H, aryl), 6.45–6.46 (m, 2H, aryl), 6.66–6.68 ppm (m, 4H, aryl), 6.91–6.92 (m, 2H, aryl), 7.42–7.43 (m, 2H, aryl), 7.98–8.00 (m, 2H, aryl), 8.21–8.22 (m, 2H, aryl), 9.04 (s, 2H, –N=CH–); $^{13}C\{^1H\}$ NMR (100 MHz, DMSO-d_6): δ (ppm) 54.3 (–O–CH_3), 111.8, 115.6, 115.7, 118.6, 127.3, 133.1, 134.2, 134.3, 135.3, 141.3, 151.3 (aryl), 156.1 (C=N); $^{29}Si\{^1H\}$ NMR (79.5 MHz, DMSO-d_6): δ (ppm) −165.1.

LSiPh(4-Me$_2$N-C$_6$H$_4$). A solution of H_2L (0.70 g, 2.67 mmol) and triethylamine (1.08 g, 10.7 mmol) in THF (5 mL) was stirred at room temperature, and chlorotrimethylsilane (0.70 g, 6.45 mmol) in THF (2 mL) was added dropwise via syringe. The yellow suspension thus obtained was heated to and stirred at 50 °C (3 h) and cooled to room temperature. Thereafter, the triethylamine hydrochloride precipitate was filtered off and washed with THF (5 mL). From the combined filtrate and washings the solvent was removed under reduced pressure (condensation into a cold trap). The orange residue was dissolved in THF (5 mL). In the dark and with stirring a solution of Ph(4-Me$_2$N-C$_6$H$_4$)SiCl$_2$ (0.87 g, 2.94 mmol) in THF (5 mL) was added quickly. The mixture was stored at room temperature in the dark for 3 days. The orange crystals obtained were filtered off, washed with THF (2 mL) and briefly dried in vacuum. Yield: 0.64 g (1.15 mmol, 43%) of LSiPh(4-Me$_2$N-C$_6$H$_4$)· THF. This composition was concluded from the crystallographic data. Elemental analysis suggests a somewhat lower THF content (0.9 THF), loss of solvent may have occurred during sample preparation. Elemental analysis for $C_{33.6}H_{34.2}N_5O_{0.9}Si$ (550.55 g· mol^{-1}): C, 73.30%; H, 6.26%; N, 12.72%; found C, 72.70%; H, 6.15%; N, 21.91%. ^{1}H NMR (400 MHz, DMSO-d_6): δ (ppm) 2.59 (s, 6H, –NMe$_2$), 6.10–6.12 (m, 2H, aryl), 6.44–6.90 (mm, 12H, aryl), 7.41–7.43 (m, 2H, aryl), 7.98–8.00 (m, 2H, aryl), 8.21–8.23 (m, 3H, aryl), 9.03 (s, 2H, –N=CH–). ^{13}C{^{1}H} NMR (100 MHz, DMSO-d_6): δ (ppm) 40.1 (–NMe$_2$), 111.3, 114.6, 115.9, 119.0, 124.3, 126.4, 126.8, 131.9, 133.0, 133.8, 134.4, 135.3, 138.8, 144.8, 147.6 (aryl), 160.1 (C=N). ^{29}Si{^{1}H} NMR (79.5 MHz, DMSO-d_6): δ (ppm) −164.4.

4. Conclusions

The silicon compounds LSiPh$_2$, LSi(Anis)$_2$, LSiPh(4-Me$_2$N-C$_6$H$_4$), LSiPhCl and LSiCl$_2$, with the dianionic tetradentate (*N*,*N*′,*N*′,*N*)-chelating ligand obtained from *o*-phenylenediamine and pyrrole-2-carbaldehyde, exhibit *trans*-disposed monodentate substituents and an almost planar arrangement of the tetradentate chelator. For LSiPh$_2$, LSi(Anis)$_2$ and LSiPh(4-Me$_2$N-C$_6$H$_4$), this was concluded from the crystal structures, and for LSiPhCl and LSiCl$_2$, the corresponding molecular structures were predicted by computational methods. With respect to this configurational feature, the herein presented complexes are related to both the group of hexacoordinate Si-complexes with salen-type (*O*,*N*,*N*,*O*)-ligands, which also exhibit *trans*-arrangement of their monodentate substituents, and to hexacoordinate Si-complexes with macrocyclic (*N*,*N*,*N*,*N*)-ligands, such as phthalocyanines and porphyrines. Moreover, compounds LSiPh$_2$, LSi(Anis)$_2$, LSiPh(4-Me$_2$N-C$_6$H$_4$), LSiPhCl and LSiCl$_2$ exhibit almost perfect charge delocalization within the pyrrolide/imine chelating moiety, which results in very similar Si–N bond lengths within one molecule. Whereas this structural feature makes them appear related to phthalocyanine and prophyrine complexes, the ^{29}Si NMR characteristics (e.g., chemical shift range and orientation of the chemical shift anisotropy tensor of LSiPh$_2$) are similar to those of Si-salen-complexes. Like their salen-chelated relatives, compounds such as LSiPh$_2$ are light sensitive. In sharp contrast, upon irradiation they do not form distinct rearrangement products like the related salen-complexes (even though it would be thermodynamically allowed). Moreover, analysis of the development of bond lengths and natural charges upon altering the monodentate substituents R and R′ in compounds LSiRR′ indicates that enhanced electron withdrawing effects of R/R′ do not enhance charge separation between R/R′ and Si but lead to better charge compensation by bond shortening. This effect is observed for the tetradentate ligand as well. In the case of two different *trans*-disposed monodentate substituents (in LSiPh(4-Me$_2$N-C$_6$H$_4$) and LSiPhCl), we have not found "push-pull effects" of charges (enhanced negative charge of one group at the expense of negative charge of the other *trans*-disposed group).

Supplementary Materials: The following are available online at www.mdpi.com/2304-6740/4/2/8/s1, Figures S1–S9 and Tables S1–S9 containing graphical representations and Cartesian coordinates, respectively, of the optimized molecular structures of LSiPh$_2$, LSi(Anis)$_2$, LSiPh(4-Me$_2$N-C$_6$H$_4$), LSiPhCl, LSiCl$_2$, L^{Ph}SiPh, L^{Anis}SiAnis, L^{Ph}Si(4-Me$_2$N-C$_6$H$_4$) and L$^{(4\text{-Me2N-C6H4})}$SiPh.

Acknowledgments: We are grateful to Ute Groß for performing elemental analyses and to Beate Kutzner and Katrin Krupinski for solution NMR spectroscopic measurements.

Author Contributions: Daniela Gerlach and Jörg Wagler conceived and designed the experiments; Daniela Gerlach performed the experiments (syntheses) and computational analyses; Daniela Gerlach and Jörg Wagler performed the single-crystal X-ray diffraction analyses; Erica Brendler performed the solid-state NMR spectroscopic analyses; and Jörg Wagler wrote the paper.

Conflicts of Interest: The authors declare no conflict of interest.

References

1. Fester, G.W.; Wagler, J.; Brendler, E.; Kroke, E. Stable trichlorosilane-pyridine adducts. *Eur. J. Inorg. Chem.* **2008**, *2008*, 5020–5023. [CrossRef]
2. Fester, G.W.; Wagler, J.; Brendler, E.; Böhme, U.; Roewer, G.; Kroke, E. Octahedral adducts of dichlorosilane with substituted pyridines: Synthesis, reactivity and a comparison of their structures and ^{29}Si NMR chemical shifts. *Chem. Eur. J.* **2008**, *14*, 3164–3176. [CrossRef] [PubMed]
3. Fester, G.W.; Wagler, J.; Brendler, E.; Böhme, U.; Gerlach, D.; Kroke, E. Octahedral $HSiCl_3$ and $HSiCl_2Me$ adducts with pyridines. *J. Am. Chem. Soc.* **2009**, *131*, 6855–6864. [CrossRef] [PubMed]
4. Couzijn, E.P.A.; Slootweg, J.C.; Ehlers, A.W.; Lammertsma, K. Pentaorganosilicates. *Z. Anorg. Allg. Chem.* **2009**, *635*, 1273–1278. [CrossRef]
5. Couzijn, E.P.A.; Ehlers, A.W.; Schakel, M.; Lammertsma, K. Electronic structure and stability of pentaorganosilicates. *J. Am. Chem. Soc.* **2006**, *128*, 13634–13639. [CrossRef] [PubMed]
6. Deerenberg, S.; Schakel, M.; de Keijzer, A.H.J.F.; Kranenburg, M.; Lutz, M.; Spek, A.L.; Lammertsma, K. Tetraalkylammonium pentaorganosilicates: The first highly stable silicates with five hydrocarbon ligands. *Chem. Commun.* **2002**, 348–349. [CrossRef]
7. Wagler, J.; Böhme, U.; Brendler, E.; Blaurock, S.; Roewer, G. Novel hexacoordinate diorganosilanes with salen-type ligands: Molecular structure *versus* ^{29}Si NMR chemical shifts. *Z. Anorg. Allg. Chem.* **2005**, *631*, 2907–2913. [CrossRef]
8. Wagler, J.; Böhme, U.; Roewer, G. Activation of Si–Si bond by hypercoordination—Cleavage of a disilane and formation of a Si–C bond. *Organometallics* **2004**, *23*, 6066–6069. [CrossRef]
9. Wagler, J.; Doert, T.; Roewer, G. Synthesis of amines from imines in the coordination sphere of silicon—Surprising photo-rearrangement of hexacoordinate organosilanes. *Angew. Chem. Int. Ed.* **2004**, *43*, 2441–2444. [CrossRef] [PubMed]
10. Wagler, J.; Roewer, G. Syntheses of allyl- and 3-silylpropyl-substituted salen-like tetradentate ligands via Hypercoordinate silicon complexes. *Z. Naturforschung B* **2006**, *61*, 1406–1412.
11. Wagler, J.; Roewer, G.; Gerlach, D. Photo-driven Si–C bond cleavage in hexacoordinate silicon complexes. *Z. Anorg. Allg. Chem.* **2009**, *635*, 1279–1287. [CrossRef]
12. Kano, N.; Yamamura, M.; Kawashima, T. Reactivity control of an allylsilane bearing a 2-(phenylazo)phenyl group by photoswitching of the coordination number of silicon. *J. Am. Chem. Soc.* **2004**, *126*, 6250–6251. [CrossRef] [PubMed]
13. Kalikhman, I.; Gostevskii, B.; Kertsnus, E.; Deuerlein, S.; Stalke, D.; Botoshansky, M.; Kost, D. Competing reactions of hypercoordinate silicon dichelates. *J. Phys. Org. Chem.* **2008**, *21*, 1029–1034. [CrossRef]
14. Kertsnus-Banchik, E.; Kalikhman, I.; Gostevskii, B.; Deutsch, Z.; Botoshansky, M.; Kost, D. Hydride migration from silicon to an adjacent unsaturated imino carbon: Intramolecular hydrosilylation. *Organometallics* **2008**, *27*, 5285–5294. [CrossRef]
15. Novak, M.; Dostal, L.; Turek, J.; Alonso, M.; de Proft, F.; Ruzicka, A.; Jambor, R. Spontaneous double hydrometallation induced by N→M coordination in organometallic hydrides of Group 14 elements. *Chem. Eur. J.* **2016**, in print. [CrossRef] [PubMed]
16. Novak, M.; Dostal, L.; Alonso, M.; de Proft, F.; Ruzicka, A.; Lycka, A.; Jambor, R. Hydrosilylation induced by N→Si intramolecular coordination: Spontaneous transformation of organosilane into 1-aza-silole-type molecules in the absence of a catalyst. *Chem. Eur. J.* **2014**, *20*, 2542–2550. [CrossRef] [PubMed]
17. Yamamura, M.; Kano, N.; Kawashima, T.; Matsumoto, T.; Harada, J.; Ogawa, K. Crucial role of N···Si interactions in the solid-state coloration of disilylazobenzenes. *J. Org. Chem.* **2008**, *73*, 8244–8249. [CrossRef] [PubMed]
18. Wagler, J.; Gerlach, D.; Böhme, U.; Roewer, G. Intramolecular inter-ligand charge transfer in hexacoordinate silicon complexes. *Organometallics* **2006**, *25*, 2929–2933. [CrossRef]

19. Wagler, J.; Roewer, G. Intramolecular interligand charge transfer and a red hexacoordinate Si-complex with salen-type ligand *vs.* colorless tetracoordinate salen-Si-complexes with similar substituents. *Inorg. Chim. Acta* **2007**, *360*, 1717–1724. [CrossRef]
20. Gerlach, D.; Ehlers, A.W.; Lammertsma, K.; Wagler, J. Silicon(IV) chelates of an (ONN′)-tridentate pyrrole-2-carbaldimine ligand: Syntheses, structures and UV/Vis properties. *Z. Naturforschung B* **2009**, *64*, 1571–1579. [CrossRef]
21. Wagler, J.; Brendler, E. Metallasilatranes: Palladium(II) and platinum(II) as lone-pair donors to silicon(IV). *Angew. Chem. Int. Ed.* **2010**, *49*, 624–627. [CrossRef] [PubMed]
22. Truflandier, L.A.; Brendler, E.; Wagler, J.; Autschbach, J. ^{29}Si DFT/NMR observation of spin-orbit effect in metallasilatrane sheds some light on the strength of the metal→Si interaction. *Angew. Chem. Int. Ed.* **2011**, *50*, 255–259. [CrossRef] [PubMed]
23. Autschbach, J.; Sutter, K.; Truflandier, L.A.; Brendler, E.; Wagler, J. Atomic contributions from spin-orbit coupling to ^{29}Si NMR chemical shifts in metallasilatrane complexes. *Chem. Eur. J.* **2012**, *18*, 12803–12813. [CrossRef] [PubMed]
24. Wahlicht, S.; Brendler, E.; Heine, T.; Zhechkov, L.; Wagler, J. 7-Azaindol-1-yl(organo)silanes and their $PdCl_2$ complexes: Pd-capped tetrahedral silicon coordination spheres and paddlewheels with a Pd–Si axis. *Organometallics* **2014**, *33*, 2479–2488. [CrossRef]
25. Gualco, P.; Mallet-Ladeira, S.; Kameo, H.; Nakazawa, H.; Mercy, M.; Maron, L.; Amgoune, A.; Bourissou, D. Coordination of a triphosphine-silane to gold: Formation of a trigonal pyramidal complex featuring Au→Si interaction. *Organometallics* **2015**, *34*, 1449–1453. [CrossRef]
26. Kameo, H.; Kawamoto, T.; Bourissou, D.; Sakaki, S.; Nakazawa, H. Evaluation of the σ-donation from group 11 metals (Cu, Ag, Au) to silane, germane, and stannane based on the experimental/theoretical systematic approach. *Organometallics* **2015**, *34*, 1440–1448. [CrossRef]
27. Gualco, P.; Mercy, M.; Ladeira, S.; Coppel, Y.; Maron, L.; Amgoune, A.; Bourissou, D. Hypervalent silicon compounds by coordination of diphosphine-silanes to gold. *Chem. Eur. J.* **2010**, *16*, 10808–10817. [CrossRef] [PubMed]
28. Sun, J.; Ou, C.; Wang, C.; Uchiyama, M.; Deng, L. Silane-functionalized *N*-heterocyclic carbene-cobalt complexes containing a five-coordinate silicon with a covalent Co–Si bond. *Organometallics* **2015**, *34*, 1546–1551. [CrossRef]
29. Junold, K.; Baus, J.A.; Burschka, C.; Vent-Schmidt, T.; Riedel, S.; Tacke, R. Five-coordinate silicon(II) compounds with Si–M bonds (M = Cr, Mo, W, Fe): Bis[*N*,*N*′-diisopropylbenzamidinato(−)]silicon(II) as a ligand in transition-metal complexes. *Inorg. Chem.* **2013**, *52*, 11593–11599. [CrossRef] [PubMed]
30. Wagler, J.; Brendler, E.; Heine, T.; Zhechkov, L. Disilicon complexes with two hexacoordinate Si atoms: Paddlewheel-shaped isomers with (ClN_4)Si-Si(S_4Cl) and (ClN_2S_2)Si-Si(S_2N_2Cl) skeletons. *Chem. Eur. J.* **2013**, *19*, 14296–14303. [CrossRef] [PubMed]
31. Wagler, J.; Brendler, E.; Langer, T.; Pöttgen, R.; Heine, T.; Zhechkov, L. Ylenes in the M^{II}→Si^{IV} (M = Si, Ge, Sn) coordination mode. *Chem. Eur. J.* **2010**, *16*, 13429–13434. [CrossRef] [PubMed]
32. Wächtler, E.; Gericke, R.; Kutter, S.; Brendler, E.; Wagler, J. Molecular structures of pyridinethiolato complexes of Sn(II), Sn(IV), Ge(IV), and Si(IV). *Main Group Met. Chem.* **2013**, *36*, 181–191. [CrossRef]
33. Levason, W.; Pugh, D.; Reid, G. Phosphine and diphosphine complexes of silicon(IV) halides. *Inorg. Chem.* **2013**, *52*, 5185–5193. [CrossRef] [PubMed]
34. Weiss, J.; Theis, B.; Baus, J.A.; Burschka, C.; Bertermann, R.; Tacke, R. Neutral pentacoordinate silicon(IV) complexes with a tridentate dianionic *O*,*N*,*O* or *N*,*N*,*O* ligand, an anionic PhX ligand (X = O, S, Se), and a phenyl group: Synthesis and structural characterization in the solid state and in solution. *Z. Anorg. Allg. Chem.* **2014**, *640*, 300–309. [CrossRef]
35. Baus, J.A.; Burschka, C.; Bertermann, R.; Fonseca Guerra, C.; Bickelhaupt, F.M.; Tacke, R. Neutral six-coordinate and cationic five-coordinate silicon(IV) complexes with two bidentate monoanionic *N*,*S*-pyridine-2-thiolato(−) ligands. *Inorg. Chem.* **2013**, *52*, 10664–10676. [CrossRef] [PubMed]
36. Junold, K.; Baus, J.A.; Burschka, C.; Auerhammer, D.; Tacke, R. Stable five-coordinate silicon(IV) complexes with SiN_4X skeletons (X = S, Se, Te) and Si:X double bonds. *Chem. Eur. J.* **2012**, *18*, 16288–16291. [CrossRef] [PubMed]

37. Kobelt, C.; Burschka, C.; Bertermann, R.; Fonseca Guerra, C.; Bickelhaupt, F.M.; Tacke, R. Synthesis and structural characterisation of neutral pentacoordinate silicon(IV) complexes with a tridentate dianionic *N*,*N*,*S* chelate ligand. *Dalton Trans.* **2012**, *41*, 2148–2162. [CrossRef] [PubMed]
38. Marckwordt, A.; Rajasekharan-Nair, R.; Steel, G.; Kennedy, A.R.; Reglinski, J.; Spicer, M.D. The first structurally characterised example of silicon in an S6 coordination sphere. *Eur. J. Inorg. Chem.* **2016**, in print. [CrossRef]
39. Mutneja, R.; Singh, R.; Kaur, V.; Wagler, J.; Fels, S.; Kroke, E. Schiff base tailed silatranes for the fabrication of functionalized silica based magnetic nano-cores possessing active sites for the adsorption of copper ions. *New J. Chem.* **2016**, *40*, 1640–1648. [CrossRef]
40. Liberman-Martin, A.L.; Bergman, R.G.; Tilley, T.D. Lewis acidity of bis(perfluorocatecholato)silane: Aldehyde hydrosilylation catalyzed by a neutral silicon compound. *J. Am. Chem. Soc.* **2015**, *137*, 5328–5331. [CrossRef] [PubMed]
41. Li, J.; Li, Y.; Purushothaman, I.; de, S.; Li, B.; Zhu, H.; Parameswaran, P.; Ye, Q.; Liu, W. Fine tuning of the substituents on the *N*-geminal phosphorus/silicon-based lewis pairs for the synthesis of *Z*-Type silyliminophosphoranylalkenes. *Organometallics* **2015**, *34*, 4209–4217. [CrossRef]
42. Ignatyev, I.S.; Kochina, T.A.; Avrorin, V.V.; Gurzhiy, V.V.; Fundamensky, V.S. Molecular and crystal structures of 2-phenyl-2-hydro-6-methyl-1,3-dioxa-6-aza-2-silacyclooctane. *J. Mol. Struct.* **2015**, *1094*, 169–173. [CrossRef]
43. Sterkhova, I.V.; Lazarev, I.M.; Smirnov, V.I.; Lazareva, N. 1-(Methylaminomethyl)silatrane: Synthesis, characterization and reactivity. *J. Organomet. Chem.* **2015**, *775*, 27–32. [CrossRef]
44. Maguylo, C.; Chukwu, C.; Aun, M.; Monroe, T.B.; Ceccarelli, C.; Jones, D.S.; Merkert, J.W.; Donovan-Merkert, B.T.; Schmedake, T.A. Exploring the structure and redox activity of hexacoordinate bis(bipyridyl)silicon(IV) complexes. *Polyhedron* **2015**, *94*, 52–58. [CrossRef]
45. Waerder, B.; Steinhauer, S.; Bader, J.; Neumann, B.; Stammler, H.-G.; Vishnevskiy, Y.V.; Hoge, B.; Mitzel, N.W. Pentafluoroethyl-substituted α-silanes: Model compounds for new insights. *Dalton Trans.* **2015**, *44*, 13347–13358. [CrossRef] [PubMed]
46. Mueck, F.M.; Baus, J.A.; Nutz, M.; Burschka, C.; Poater, J.; Bickelhaupt, F.M.; Tacke, R. Reactivity of the donor-stabilized silylenes [iPrNC(Ph)NiPr]$_2$Si and [iPrNC(NiPr$_2$)NiPr]$_2$Si: Activation of CO_2 and CS_2. *Chem. Eur. J.* **2015**, *21*, 16665–16672. [CrossRef] [PubMed]
47. Mueck, F.M.; Kloss, D.; Baus, J.A.; Burschka, C.; Bertermann, R.; Poater, J.; Fonseca Guerra, C.; Bickelhaupt, F.M.; Tacke, R. Stable four-coordinate guanidinatosilicon(IV) complexes with SiN_3El skeletons (El = S, Se, Te) and Si=El double bonds. *Chem. Eur. J.* **2015**, *21*, 14011–14021. [CrossRef] [PubMed]
48. Tacke, R.; Kobelt, C.; Baus, J.A.; Bertermann, R.; Burschka, C. Synthesis, structure and reactivity of a donor-stabilized silylene with a bulky bidentate benzamidinato ligand. *Dalton Trans.* **2015**, *44*, 14959–14974. [CrossRef] [PubMed]
49. Duggal, P. Synthesis, characterization and quantum mechanical calculations of five coordinated anionic silicates. *J. Chem. Biol. Phys. Sci.* **2016**, *6*, 153–164.
50. Singh, G.; Promila; Saroa, A.; Singh, J.; Sharm, R.P.; Ferretti, V. Schiff base functionalized Organopropylsilatranes: Synthesis and structural characterization. *J. Chem. Sci.* **2016**, *128*, 193–200. [CrossRef]
51. Chipanina, N.N.; Lazareva, N.F.; Oznobikhina, L.P.; Lazarev, I.M.; Shainyan, B.A. The hydrolysis of (O–Si)-chelate [*N*-(acetamido)methyl]dimethylchlorosilanes. DFT and MP2 study, QTAIM and NBO analysis. *Comput. Theor. Chem.* **2015**, *1070*, 162–173. [CrossRef]
52. Singh, G.; Rani, S.; Saroa, A.; Girdhar, S.; Singh, J.; Arora, A.; Aulakh, D.; Wriedt, M. Organosilatranes with thioester-anchored heterocyclic ring assembly: Cu^{2+} ion binding and fabrication of hybrid silica nanoparticles. *RSC Adv.* **2015**, *5*, 65963–65974. [CrossRef]
53. Doronina, E.P.; Sidorkin, V.F.; Lazareva, N.F. Analysis of the hypersensitivity of the ^{29}Si NMR chemical shift of the pentacoordinate silicon compounds to the temperature effect. *N*-(Silylmethyl)acetamides. *J. Phys. Chem. A* **2015**, *119*, 3663–3673. [CrossRef] [PubMed]
54. Matsuoka, D.; Nishigaichi, Y. Allyl-transfer reaction from photoexcited hypervalent allylsilicon reagent toward dicyanobenzenes. *Chem. Lett.* **2015**, *44*, 163–165. [CrossRef]
55. Kano, N.; Miyake, H.; Sasaki, K.; Kawashima, T. Oxidative bond cleavage of the silicon–silicon bond of a pentacoordinated disilicate. *Heteroat. Chem.* **2015**, *26*, 183–186. [CrossRef]

56. Schwarzer, A.; Fels, S.; Boehme, U. Two reversible enantiotropic phase transitions in a pentacoordinate silicon complex with an *O*,*N*,*O*′-tridentate valinate ligand. *Acta Crystallogr. C* **2015**, *71*, 511–516. [CrossRef] [PubMed]
57. Aghazadeh Meshgi, M.; Baumgartner, J.; Marschner, C. Oligosilanylsilatranes. *Organometallics* **2015**, *34*, 3721–3731. [CrossRef] [PubMed]
58. Boettcher, T.; Steinhauer, S.; Lewis-Alleyne, L.C.; Neumann, B.; Stammler, H.-G.; Bassil, B.S.; Roeschenthaler, G.-V.; Hoge, B. NHC→$SiCl_4$: An ambivalent carbene-transfer reagent. *Chem. Eur. J.* **2015**, *21*, 893–899. [CrossRef] [PubMed]
59. Kost, D.; Kalikhman, I. Hypercoordinate silicon complexes based on hydrazide ligands. A remarkably flexible molecular system. *Acc. Chem. Res.* **2009**, *42*, 303–314. [CrossRef] [PubMed]
60. Levason, W.; Reid, G.; Zhang, W. Coordination complexes of silicon and germanium halides with neutral ligands. *Coord. Chem. Rev.* **2011**, *255*, 1319–1341. [CrossRef]
61. Wagler, J.; Böhme, U.; Kroke, E. Higher-coordinated molecular silicon compounds. In *Structure and Bonding*; Scheschkewitz, D., Ed.; Springer: Berlin, Germany, 2014; Volume 155, pp. 29–105.
62. Korlyukov, A.A. Coordination compounds of tetravalent silicon, germanium and tin: The structure, chemical bonding and intermolecular interactions in them. *Russ. Chem. Rev.* **2015**, *84*, 422–440. [CrossRef]
63. Peloquin, D.M.; Schmedake, T.A. Recent advances in hexacoordinate silicon with pyridine-containing ligands: Chemistry and emerging applications. *Coord. Chem. Rev.* **2016**, in print. [CrossRef]
64. Gerlach, D.; Brendler, E.; Heine, T.; Wagler, J. Dianion of pyrrole-2-*N*-(o-hydroxyphenyl)carbaldimine as an interesting tridentate (ONN) ligand system in hypercoordinate silicon complexes. *Organometallics* **2007**, *26*, 234–240. [CrossRef]
65. Wagler, J. A Disilane with a hypercoordinate silicon atom: Coordination of an imine ligand *versus* Si–Si bond splitting. *Organometallics* **2007**, *26*, 155–159. [CrossRef]
66. Wagler, J.; Brendler, E. Hypercoordinate diorganosilanes featuring an (ONO) tridentate ligand. A surprising equilibrium between penta- and tetracoordination. *Z. Naturforschung B* **2007**, *62*, 225–234.
67. Wagler, J.; Gerlach, D.; Roewer, G. 2-*N*-(Quinoline-8-yl)iminomethylphenolate—A (ONN)-tridentate ligand system in silicon complex chemistry. *Inorg. Chim. Acta* **2007**, *360*, 1935–1942. [CrossRef]
68. Wagler, J.; Hill, A.F. Templated rearrangement of silylated benzoxazolin-2-ones: A novel tridentate $(ONO)^{2-}$ chelating ligand system. *Organometallics* **2007**, *26*, 3630–3632. [CrossRef]
69. Lippe, K.; Gerlach, D.; Kroke, E.; Wagler, J. *N*-(*o*-Aminophenyl)-2-oxy-4-methoxybenzophenoneimine—Si-chelation by a tridentate *ONN* ligand system *versus* benzimidazoline formation. *Inorg. Chem. Commun.* **2008**, *11*, 492–496. [CrossRef]
70. Kämpfe, A.; Kroke, E.; Wagler, J. Hypercoordinate silicon complexes of (*ONN*′ *vs.* *ONO*′) Schiff base type *N*-(2-carbamidophenyl)imines: Examples for exclusively *O*-silylated carbamides. *Eur. J. Inorg. Chem.* **2009**, *2009*, 1027–1035. [CrossRef]
71. Gericke, R.; Gerlach, D.; Wagler, J. Ring-strain-formation Lewis-acidity? A pentacoordinate silacyclobutane comprising exclusively equatorial Si–C bonds. *Organometallics* **2009**, *28*, 6831–6834. [CrossRef]
72. Schwarz, D.; Brendler, E.; Kroke, E.; Wagler, J. Pentacoordinate silicon complexes with *N*-(2-pyridylmethyl)salicylamide as a dianionic (*ONN*′) tridentate chelator. *Z. Anorg. Allg. Chem.* **2012**, *638*, 1768–1775. [CrossRef]
73. Wagler, J.; Böhme, U.; Roewer, G. Silicon-enamine complexes: Pentacoordinate silicon compounds. *Angew. Chem. Int. Ed.* **2002**, *41*, 1732–1734. [CrossRef]
74. Wagler, J.; Böhme, U.; Brendler, E.; Roewer, G. First X-ray structure of a cationic silicon complex with salen-type ligand: An unusual compound with two different Si–N dative bonds. *Z. Naturforschung B* **2004**, *59*, 1348–1352.
75. Wagler, J.; Roewer, G. First X-ray structures of ethylene bridged neutral dimeric hexacoordinate silicon complexes with tetradentate salen-type ligands. *Z. Naturforschung B* **2005**, *60*, 709–714.
76. Wagler, J.; Böhme, U.; Brendler, E.; Thomas, B.; Goutal, S.; Mayr, H.; Kempf, B.; Remennikov, B.Y.; Roewer, G. Switching between penta- and hexacoordination with salen-silicon-complexes. *Inorg. Chim. Acta* **2005**, *358*, 4270–4286. [CrossRef]
77. Lippe, K.; Gerlach, D.; Kroke, E.; Wagler, J. Hypercoordinate organosilicon complexes of an *ONN*′*O*′ chelating ligand: Regio- and diastereoselectivity of rearrangement reactions in Si-salphen-systems. *Organometallics* **2009**, *28*, 621–629. [CrossRef]

78. Kane, K.M.; Lorenz, C.R.; Heilman, D.M.; Lemke, F.R. Substituent effects on the spectroscopic properties and reactivity of hexacoordinate silicon(IV) porphyrin complexes. *Inorg. Chem.* **1998**, *37*, 669–673. [CrossRef]
79. Zheng, J.-Y.; Konishi, K.; Aida, T. Crystallographic studies of organosilicon porphyrins: Stereoelectronic effects of axial groups on the nonplanarity of the porphyrin ring. *Inorg. Chem.* **1998**, *37*, 2591–2594. [CrossRef]
80. Ishida, S.; Yoshimura, K.; Matsumoto, H.; Kyushin, S. Selective Si–C bond cleavage on a diorganosilicon porphyrin complex bearing different axial ligands. *Chem. Lett.* **2009**, *38*, 362–363. [CrossRef]
81. Taskin, G.C.; Durmus, M.; Yüksel, F.; Mantareva, V.; Kussovski, V.; Angelov, I.; Atilla, D. Axially paraben substituted silicon(IV) phthalocyanines towards dental pathogen Streptococcus mutans: Synthesis, photophysical, photochemical and *in vitro* properties. *J. Photochem. Photobiol. A* **2015**, *306*, 31–40. [CrossRef]
82. Kämpfe, A.; Kroke, E.; Wagler, J. Silicon compounds of 1,1-bis(pyrrol-2-yl)ethenes: Molecular structures and chemical and spectroscopic properties. *Organometallics* **2014**, *33*, 112–120. [CrossRef]
83. Kämpfe, A.; Brendler, E.; Kroke, E.; Wagler, E. 2-Acylpyrroles as mono-anionic *O*,*N*-chelating ligands in silicon coordination chemistry. *Chem. Eur. J.* **2014**, *20*, 9409–9418. [CrossRef] [PubMed]
84. Kämpfe, A.; Brendler, E.; Kroke, E.; Wagler, J. Tp*Cu(I)–CN–SiL_2–NC–Cu(I)Tp*—A hexacoordinate Si-complex as connector for redox active metals via π-conjugated ligands. *Dalton Trans.* **2015**, *44*, 4744–4750. [CrossRef] [PubMed]
85. Munro, O.Q.; Joubert, S.D.; Grimmer, C.D. Molecular recognition: Preorganization of a bis(pyrrole) Schiff base derivative for tight dimerization by hydrogen bonding. *Chem. Eur. J.* **2006**, *12*, 7987–7999. [CrossRef] [PubMed]
86. Wächtler, E.; Kämpfe, A.; Krupinski, K.; Gerlach, D.; Kroke, E.; Brendler, E.; Wagler, J. New Insights into hexacoordinated silicon complexes with 8-oxyquinolinato ligands: 1,3-Shift of Si-bound hydrocarbyl substituents and the influence of Si-bound halides on the 8-oxyquinolinate coordination features. *Z. Naturforschung B* **2014**, *69*, 1402–1418. [CrossRef]
87. Kost, D.; Kingston, V.; Gostevskii, B.; Ellern, A.; Stalke, D.; Walfort, B.; Kalikhman, I. Donor-stabilized silyl cations. 3. Ionic dissociation of hexacoordinate silicon complexes to pentacoordinate siliconium salts driven by ion solvation. *Organometallics* **2002**, *21*, 2293–2305. [CrossRef]
88. Mason, J. Conventions for the reporting of nuclear magnetic shielding (or shift) tensors suggested by participants in the NATO ARW on NMR Shielding Constants at the University of Maryland, College Park, July 1992. *Solid State Nucl. Magn. Reson.* **1993**, *2*, 285–288. [CrossRef]
89. Herzfeld, J.; Berger, A.E. Sideband intensities in NMR spectra of sample spinning at the magic angle. *J. Chem. Phys.* **1980**, *73*, 6021–6030. [CrossRef]
90. Brendler, E.; Wächtler, E.; Wagler, J. Hypercoordinate silacycloalkanes: Step-by-step tuning of N→Si Interactions. *Organometallics* **2009**, *28*, 5459–5465. [CrossRef]
91. Sheldrick, G.M. *Shelxs-97, Program for the Solution of Crystal Structures*; version WinGX© (release 97-2) 1993–1997; University of Göttingen: Göttingen, Germany, 1997.
92. Sheldrick, G.M. *Shelxl-97, Program for the Refinement of Crystal Structures*; version WinGX© (release 97-2) 1993–1997; University of Göttingen: Göttingen, Germany, 1997.
93. Sheldrick, G.M. A short history of SHELX. *Acta Crystallogr.* **2008**, *A64*, 112–122. [CrossRef] [PubMed]
94. Farrugia, L.J. ORTEP-3 for windows—A version of ORTEP-III with a graphical user interface (GUI). *J. Appl. Crystallogr.* **1997**, *30*, 565. [CrossRef]
95. *POV-RAY*; version 3.6.2. Trademark of Persistence of Vision Raytracer Pty. Ltd.: Williamstown, Victoria, Australia Copyright Hallam Oaks Pty. Ltd., 1994–2004. Available online: http://www.povray.org/download/ (accessed on 22 December 2011).
96. Frisch, M.J.; Trucks, G.W.; Schlegel, H.B.; Scuseria, G.E.; Robb, M.A.; Cheeseman, J.R.; Scalmani, G.; Barone, V.; Mennucci, B.; Petersson, G.A.; *et al. Gaussian 09*; revision D.01; Gaussian, Inc.: Wallingford, CT, USA, 2009.
97. Hohenberg, P.; Kohn, W. Inhomogeneous electron gas. *Phys. Rev.* **1964**, *136*, B864–B871. [CrossRef]
98. Kohn, W.; Sham, L.J. Self-consistent equations including exchange and correlation effects. *Phys. Rev.* **1965**, *140*, A1133–A1138. [CrossRef]
99. Parr, R.G.; Yang, W. *Density-Functional Theory of Atoms and Molecules*; Oxford University Press: Oxford, UK, 1989.
100. Adamo, C.; Barone, V. Exchange functionals with improved long-range behavior and adiabatic connection methods without adjustable parameters: The mPW and mPW1PW models. *J. Chem. Phys.* **1998**, *108*, 664–675. [CrossRef]

101. McLean, A.D.; Chandler, G.S. Contracted Gaussian basis sets for molecular calculations. I. Second row atoms, Z = 11–18. *J. Chem. Phys.* **1980**, *72*, 5639–5648. [CrossRef]
102. Raghavachari, K.; Binkley, J.S.; Seeger, R.; Pople, J.A. Self-consistent molecular orbital methods. XX. A basis set for correlated wave functions. *J. Chem. Phys.* **1980**, *72*, 650–654.
103. Foster, J.P.; Weinhold, F. Natural hybrid orbitals. *J. Am. Chem. Soc.* **1980**, *102*, 7211–7218. [CrossRef]
104. Reed, A.E.; Weinhold, F. Natural bond orbital analysis of near-Hartree-Fock water dimer. *J. Chem. Phys.* **1983**, *78*, 4066–4073. [CrossRef]
105. Reed, A.E.; Weinstock, R.B.; Weinhold, F. Natural population analysis. *J. Chem. Phys.* **1985**, *83*, 735–746. [CrossRef]
106. Reed, A.E.; Weinhold, F. Natural localized molecular orbitals. *J. Chem. Phys.* **1985**, *83*, 1736–1740. [CrossRef]
107. Carpenter, J.E.; Weinhold, F. Analysis of the geometry of the hydroxymethyl radical by the "different hybrids for different spins" natural bond orbital procedure. *J. Mol. Struct. THEOCHEM* **1988**, *46*, 41–62. [CrossRef]
108. Reed, A.E.; Curtiss, L.A.; Weinhold, F. Intermolecular interactions from a natural bond orbital, donor–acceptor viewpoint. *Chem. Rev.* **1988**, *88*, 899–926. [CrossRef]
109. Weinhold, F.; Carpenter, J.E. *The Structure of Small Molecules and Ions*; Naaman, R., Vager, Z., Eds.; Plenum: New York, NY, USA, 1988; pp. 227–236.
110. Head-Gordon, M.; Pople, J.A.; Frisch, M.J. MP2 energy evaluation by direct methods. *Chem. Phys. Lett.* **1988**, *153*, 503–506. [CrossRef]
111. Saebø, S.; Almlöf, J. Avoiding the integral storage bottleneck in LCAO calculations of electron correlation. *Chem. Phys. Lett.* **1989**, *154*, 83–89. [CrossRef]
112. Frisch, M.J.; Head-Gordon, M.; Pople, J.A. A direct MP2 gradient method. *Chem. Phys. Lett.* **1990**, *166*, 275–280. [CrossRef]
113. Frisch, M.J.; Head-Gordon, M.; Pople, J.A. Semidirect algorithms for the MP2 energy and gradient. *Chem. Phys. Lett.* **1990**, *166*, 281–289. [CrossRef]
114. Head-Gordon, M.; Head-Gordon, T. Analytic MP2 frequencies without fifth-order storage. Theory and application to bifurcated hydrogen bonds in the water hexamer. *Chem. Phys. Lett.* **1994**, *220*, 122–128. [CrossRef]
115. Dunning, T.H., Jr. Gaussian basis sets for use in correlated molecular calculations. I. The atoms boron through neon and hydrogen. *J. Chem. Phys.* **1989**, *90*, 1007–1023. [CrossRef]
116. Kendall, R.A.; Dunning, T.H., Jr.; Harrison, R.J. Electron affinities of the first-row atoms revisited. Systematic basis sets and wave functions. *J. Chem. Phys.* **1992**, *96*, 6796–6806. [CrossRef]
117. Woon, D.E.; Dunning, T.H., Jr. Gaussian basis sets for use in correlated molecular calculations. III. The atoms aluminum through argon. *J. Chem. Phys.* **1993**, *98*, 1358–1371. [CrossRef]
118. Peterson, K.A.; Woon, D.E.; Dunning, T.H., Jr. Benchmark calculations with correlated molecular wave functions. IV. The classical barrier height of the H + H_2 → H_2 + H reaction. *J. Chem. Phys.* **1994**, *100*, 7410–7415. [CrossRef]
119. Wilson, A.K.; van Mourik, T.; Dunning, T.H., Jr. Gaussian basis sets for use in correlated molecular calculations. VI. Sextuple zeta correlation consistent basis sets for boron through neon. *J. Mol. Struct. THEOCHEM* **1996**, *388*, 339–349. [CrossRef]
120. Becke, A.D. Density-functional thermochemistry. III. The role of exact exchange. *J. Chem. Phys.* **1993**, *98*, 5648–5652. [CrossRef]
121. Popp, F.; Nätscher, J.B.; Daiss, J.O.; Burschka, C.; Tacke, R. The 2,4,6-trimethoxyphenyl unit as a unique protecting group for silicon in synthesis and the silylation potential of (2,4,6-trimethoxyphenyl)silanes. *Organometallics* **2007**, *26*, 6014–6028. [CrossRef]